FINAL TECHNICAL REPORT FOR GRANT NUMBER: 00-HQGR0050

LABORATORY EXPERIMENTS ON ROCK FRICTION FOCUSED ON UNDERSTANDING EARTHQUAKE MECHANICS

Terry E. Tullis

and

David L. Goldsby

Brown University
Department of Geological Sciences
Providence RI 02912-1846

Tele: (401) 863-3829
FAX: (401) 863-2058
Email: Terry_Tullis@brown.edu
Web Site. http://www.geo.brown.edu/faculty/ttullis/index.html

Program Element III - Understanding Earthquake Processes

Key Words: Laboratory studies, Source characteristics, Fault dynamics, Strong ground motion

Research supported by the U.S. Geological Survey (USGS), Department of the Interior, under USGS award number 00-HQGR0050. The views and conclusions contained in this document are those of the authors and should not be interpreted as necessarily representing the official policies, either expressed or implied, of the U.S. Government.

TECHNICAL ABSTRACT

We have conducted experiments on the friction of several rock types at intermediate slip speeds, both at elevated confining pressure and at atmospheric pressure, with applications to dynamic earthquake slip. We observe dramatic frictional weakening for displacements from tens of millimeters to greater than10 m and slip rates from 0.1 mm/s to 150 mm/s. Over this range of velocities the frictional resistance decreases nearly linearly with the log of the slip velocity. This weakening is much more dramatic than would be predicted by extrapolation of standard rate and state friction from lower velocities. The weakening is seen in quartzite, feldspar-rock, and granite; it is most pronounced for quartzite and least for granite. The rate of weakening as a function of displacement increases with increasing sliding velocity. We have also conducted time-dependent finite element calculations of the temperature that take into account the complex geometry and thermal properties of our sample assembly. The average temperatures on the sliding surface, and the local 'flash' temperatures at asperity contacts calculated using analytical solutions, suggest that the temperature is much too low for the weakening to be explained by melting. After rapid sliding, strength increases slowly with time during either stationary contact or slow slip. The temperature calculations show that during this slow strength recovery the temperature, that had been modestly elevated due to frictional heating at high speed, returns to room temperature well before the strength recovers to its low velocity value. This suggests that temperature is not the main variable responsible for the weakening. The weakening mechanism is not clear, although contributing factors may include elevated temperatures caused by shear heating and the presence of amorphous material produced by the shearing. The weakening we observe at lower slip rates than those typical for earthquakes suggest substantial weakening should be common during earthquake slip. Thus, if initial stresses are large then dynamic stress drops could be large, resulting in strong ground motions.

INTRODUCTION

This is a final technical report for USGS grant 00-HQGR0050. The grant covers a one year period, from March 1, 2000 to February 28, 2001 with a no-cost extension to August 31, 2001. We have focussed our efforts on understanding friction at rapid slip rates relevant to dynamic resistance during earthquakes. We will discuss our progress in detail below.

PUBLICATIONS RESULTING FROM THIS GRANT

Kato, N., and T.E. Tullis, A composite rate- and state-dependent law for rock friction, *Eos. Trans. Am. Geophys, Union, Fall Meeting Suppl., 81*, F1025, 2000.

Tullis, T.E., Modeling earthquake cycles using nonlinear laboratory-based constitutive laws and fast multipole methods, *Eos. Trans. Am. Geophys, Union, Fall Meeting Suppl., 81*, F1079, 2000.

Tullis, T.E., Using normal displacements to evaluate whether changes in contact area can explain the friction evolution effect, *Eos. Trans. Am. Geophys, Union, Fall Meeting Suppl., 81*, F1025, 2000.

Tullis, T.E. , J. Salmon, and N. Kato, Use of fast multipoles for earthquake modeling, *Proceedings of Second ACES Workshop, Tokyo and Hakone, Japan, Oct. 15-20, 2000,* 35-40, 2000.

Goldsby, D.L., and T.E. Tullis, Low frictional strength of quartz at subseismic slip rates, manuscript in preparation for *Geophys. Res. Lett.*, 2001.

RESULTS

Background

Earthquake slip speeds are on the order of 1 m/sec. At these high velocities significant shear heating can occur, and a variety of processes may operate that might greatly lower the shear resistance. If such dynamic weakening occurs, it could cause dynamic stress drops much larger than static drops, resulting in seismic slip propagating as self-healing slip pulses rather than as a conventional crack [*Beeler and Tullis*, 1996; *Beroza and Spudich*, 1988; *Brune*, 1970; *Brune*, 1976; *Cochard and Madariaga*, 1994; *Heaton*, 1990; *Perrin et al.*, 1994]. This has implications for the magnitude of peak seismic accelerations expected during earthquakes and thus for the amplitude of strong ground shaking. It also is important for the state of stress on the fault following an earthquake. This stress state can affect the behavior of the fault in the time interval leading up to the next earthquake, and in turn can affect the nature of premonitory accelerating slip or fluid flow that might be helpful in predicting the next earthquake. Furthermore, if dynamic weakening is large enough, then it is easier for small earthquakes to grow into large ones, and earthquake recurrence intervals should be much less regular. This is because once the rupture begins, the stress concentration at the tip of the slip zone could overcome the static friction and dynamic slip could occur with very little resistance. This fits in with the views of many concerning the unpredictability of earthquakes [*Geller et al.*, 1997].

From a completely different point of view, if we knew how dynamic fault resistance depends on slip and slip velocity, we could contemplate using the waves recorded by strong

motion seismographs to make much more physically-based inversions for fault slip and slip velocity. Presently these parameters are based on a simple [*Haskel*, 1964a; *Haskel*, 1964b; *Haskel*, 1966; *Haskel*, 1969] model of fault slip that contains no physical constraints for what can occur on the fault. The non-uniqueness of these inversions could be reduced if we had a good understanding of how fault resistance varies as earthquake slip proceeds. Incorporating more realistic constraints on fault resistance into source inversions could allow us to do a better job of using seismic observations to determine the slip and velocity distributions during an earthquake.

Slip at high speed may invoke a variety of processes that could drastically alter frictional strength. If normal stress, slip velocity, and displacement are large enough and no fluids are present, frictional melting can occur. This process has been investigated in experiments by *Spray* [1987] and by [*Tsutsumi and Shimamoto*, 1997]. If pore fluids are present, pore pressure may rise due to thermal expansion of pore fluid. The magnitude of this effect depends in part on the compressibility and thermal expansion of the fluid and of the rock matrix, and also depends critically on the permeability of the rocks along the fault zone [*Lachenbruch*, 1980; *Mase and Smith*, 1984; *Mase and Smith*, 1987]. High slip speeds may also result in dilatancy of the fault zone [*Beeler et al.*, 1996; *Marone and Kilgore*, 1993; *Segall and Rice*, 1995], which will tend to reduce pore pressure. Other proposed dynamic weakening mechanisms include acoustic fluidization [*Melosh*, 1979; *Melosh*, 1996] and reduction of dynamic normal stresses via normal vibrations [*Brune et al.*, 1993], a process that can be enhanced if the elastic properties of the rock across the fault are different [*Ben-Zion and Andrews*, 1998].

We have discovered dramatic weakening by a process that does not seem to be any of those on the above list. In this report we will describe the results to date and our attempts to understand the origin of this unexpected weakening. Whether or not this new weakening process may be important for earthquakes remains to be determined, but if it is, the significance for strong ground motions would be profound.

We will also describe our progress toward developing the capability to slide at slip rates up to seismic slip rates of 1 m/s at elevated confining pressure. Our present apparatus is limited in its slip speeds to 5 mm/s, a speed too slow to produce frictional melting. The presence of pseudotachylites along some fault surfaces shows that this is a process that clearly does operate during some earthquakes, and we plan to investigate this in future years.

Experimental Observations

We have continued our series of experiments at intermediate slip velocities to evaluate the effect that dynamic slip is likely to have on stresses during earthquakes. Although we are unable to conduct experiments at speeds of 1 m/s typical of dynamic earthquake slip, we can slide for large distances at velocities of up to 5 mm/s under confining pressure in our rotary shear apparatus, and can slide large distances at velocities up to 150 mm/s at a low normal stress of 5 MPa in an atmospheric pressure apparatus. We observe extraordinary weakening in both of these experimental configurations as is described in the sections below. We have also used a finite element model to make extensive calculations of the temperatures generated by frictional sliding in our samples.

Experiments in our rotary shear apparatus. Results from our confined and unconfined experiments on quartzite are summarized in Fig. 1. Samples were slid at 1 μm/s for the first few millimeters of slip, then at 3.2 mm/s for the remainder of each experiment. As shown in Fig. 1,

we observe a dramatic decrease in strength for confined samples deformed at normal stresses of 28 and 112 MPa; the friction coefficient decreases from an initial low speed value of 0.7 to 0.85 to a final value <0.4 over displacements approaching 3 m. Experiments on unconfined samples were also conducted in our high-pressure apparatus. In these experiments, samples are placed inside the gas pressure medium, but without the O-rings and Teflon sliding jackets that isolate the sample from the confining medium as in a confined test, rendering the samples effectively unconfined. One result of such tests is shown in Fig. 1. The friction coefficient decreases from a low speed value of 0.7-0.9 to a final value of <0.3 in ~9 m of displacement. This favorable comparison also demonstrates that the weakening is not caused by contamination from the Teflon sliding jackets.

Rapid sliding experiments under confined conditions have also been conducted on dolomite, feldspar, granite, and a quartz mica mylonite. The results of several tests for feldspar, granite, and mylonite, for a normal stress of 28 MPa, are compared with those of quartzite in Fig. 2. As shown in Fig. 2, similar albeit less dramatic weakening occurs for feldspar as for quartzite. Experiments on granite and mylonite slid at 28 MPa reveal no weakening. The granite sample slid at 112 MPa, however, shows a nearly identical weakening as quartzite slid at 28 MPa. We have also conducted rapid sliding experiments on simulated gouge layers of quartz and of granite. Slip in quartz gouge localizes and substantial weakening occurs at 28 MPa normal stress as for experiments on initially bare quartzite surfaces. Experiments on granite gouge show no weakening at 28 MPa, as is the case for initially bare granite surfaces.

Experiments at ambient pressure. We have made significant progress in a new series of experiments conducted in the Mechanical Testing Facility in the Division of Engineering at Brown University. These experiments extend our observations to higher slip rates than are currently available in our high pressure apparatus, and also confirm that weakening is not an artifact of our confined sample assembly.

The experiments of this new type were conducted in an ambient pressure Instron torsion/compression/tension apparatus. The apparatus has several advantages over our high pressure apparatus, the most important being that we easily can extend the velocity range of our experiments to those approaching earthquake slip speeds, i.e., up to ~0.5 m/s. One disadvantage of the apparatus is that we can slide in one direction to displacements of only ~40 mm. However, larger displacements can be achieved by sliding the full available range in one direction, then reversing the sliding direction and sliding again over the same displacement range in reverse. By oscillating sliding in this manner, we can achieve sliding displacements of many meters. During this grant period, we have also set up a high-speed data acquisition system with this apparatus allowing for data sampling rates of up to 1 kHz.

Results from oscillating sliding experiments in the velocity range 3 to 75 mm/s to large displacement are shown in Fig. 3. The friction reaches a steady-state level after ~1 m of slip. This steady-state friction decreases as the velocity increases. For the three velocities shown in Fig. 3, the reduction in friction from its initial value to the steady-state level is a linear function of the log of slip velocity. The magnitude of these reductions is much larger than is typically observed for rate and state friction at lower velocities, as is clearly shown in Fig. 4. It appears that there is a mechanism change at around 0.1 mm/s, indicated by the change in slope. Another mechanism change may occur at higher velocities or higher normal stress when the temperature is high enough to cause melting. As discussed below, melting does not seem possible in our

current experiments.

It is interesting to note that for velocities of 75 and 150 mm/s, the decrease in friction coefficient at short displacement is much more rapid than at lower velocities, as shown in Fig. 5. An intriguing possibility is that above a velocity of ~50 mm/s, rapid increased weakening due to thermal softening or even melting of asperities may occur, as discussed below.

Fault surface temperatures. To ascertain whether the extraordinary weakening might result from melt lubrication of the fault surface, and to determine the dependence of frictional strength on temperature, the average surface temperature of our experimental faults was calculated. To obtain an upper bound on the temperature, we assume a fault zone thickness of zero, rather than a thin but finite fault width as occurs in our experiments. Temperatures were estimated using 1) an analytical solution for a semi-infinite half space from [*Carslaw and Jaeger*, 1959], 2) a numerical solution of the equations of [*Sleep*, 1995], and 3) a finite element calculation. Method 1) assumes a constant value for the friction coefficient and a fixed velocity, and thus a constant flux of heat at the fault surface. Methods 2) and 3) use our experimental data for friction coefficient and sliding velocity as functions of time and thus a time varying flux of heat at the fault surface. 1) and 2) both yield upper bounds on the fault temperature, since the tendency for high thermal conductivity components (e.g., steel) in the sample assemblies to reduce the temperature on the fault is not considered. The finite element method allows us to include the effect of these high conductivity components and other geometrically complex parts on the fault temperature. All of our prior conclusions regarding the temperature dependence of frictional strength in our experiments have been based on temperatures calculated using methods 1) and 2). As will be demonstrated below, finite element calculations reveal that the fault surface temperatures are much less, sometimes by an order of magnitude, than indicated in the previous calculations.

The finite element mesh used to calculate fault temperature for a representative experiment is shown in Fig. 6a,b. The calculation assumes a radial geometry, with the centerline of the sample assembly along the left-hand edge of the box. A constant temperature (23 ^{o}C) boundary condition is assigned to the lower boundary of the grid and the pressure vessel wall (right edge of the box), and a zero flux boundary condition is assigned to the upper surface of the box. A time-varying flux $q = \mu(t)\, \sigma_n\, V(t)$ is applied to the fault surface, where μ is the friction coefficient, σ_n is normal stress, and V is slip velocity. The variation of temperature with time for a node near the center of the fault surface is shown in Fig. 6c.

Temperature calculations for experiments conducted in the high-pressure apparatus at several representative sliding speeds and normal stresses are shown in Fig. 7. The data indicate temperature increases for each normal stress of less than ~100 ^{o}C. Temperature calculations for several experiments conducted at higher sliding speeds but a lower normal stress of 5 MPa in the ambient pressure apparatus are shown in Fig. 8. These unconfined samples experienced temperature increases of ~60 ^{o}C or less.

These temperature calculations are in accord with estimates from thermal dyes. Dyes were applied to the outside of our sample rings as well as in 1 mm deep wells drilled into the fault surface in unconfined experiments conducted in the high pressure apparatus. The two dyes selected undergo an irreversible phase change at temperatures of 100 and 300 ^{o}C. After sliding to a displacement of 9 m at 16 MPa normal stress and 3.2 mm/s, the 100 ^{o}C dye in the well on the fault surface was transformed, whereas the 300 ^{o}C dye remained untransformed. On the

outside of the sample rings, the 100 ^{o}C dye was melted in an extremely narrow zone near the fault, and the 300 ^{o}C dye was unchanged. These observations are consistent with the temperature calculations shown in Fig. 7, which indicate a peak fault surface temperature of ~100 ^{o}C.

'Flash' temperatures. Though the average surface temperature in our experiments is insufficient for melting, transiently high temperatures higher than the average surface temperature occur at the contact junctions where energy is dissipated as heat [*Archard*, 1958; *Rice*, 1999]. These so-called 'flash' temperatures can be short-lived; at high sliding speeds on the order of m/s, flash temperatures can be of only millisecond duration [*Bowden and Tabor*, 1964]. We estimated flash temperatures in our experiments using the theory of *Archard* [1958]. The calculation assumes that circular contact junctions slide on a flat surface; the average contact junction area is determined by the applied load, the number of contacts, and the yield stress of the material (i.e., the material flows plastically at the contacts). Assuming plastic flow of contacts yields an upper bound for the temperature. Archard's analysis yields both low and high speed sliding solutions; the appropriateness of the low vs. high speed solutions is determined by the value of a dimensionless Peclet number (the ratio of the time over which heat is applied to the time required to diffuse it away).

Calculated flash temperatures using the low- and high-speed solutions and employing materials parameters for quartz are shown in Fig. 9. The Peclet number in our experiments varies from about 0.001 at V=3.2 mm/s to ~0.025 at V=75 mm/s, indicating that the low speed solution is appropriate. Thus, flash temperatures vary from <100 ^{o}C at 3 mm/s to ~1000 ^{o}C at 75 mm/s above the average background temperature. Samples slid at 75 and 150 mm/s weaken much faster at short displacement (~5 mm) than samples slid at 3 and 16 mm/s (Fig. 5), suggesting that flash heating may cause thermal weakening or even melting at the higher slip rates.

Healing with time. At the cessation of rapid sliding, the frictional strength of confined and (effectively) unconfined samples returns to pre-rapid sliding levels, as shown for unconfined samples in Fig. 10. In Fig. 10, the increase in frictional strength of two unconfined samples is shown as a function of time. At the cessation of rapid sliding, one sample was slid continuously at 1 μm/s to a total displacement of 700 mm. The other sample was slid periodically at 1 μm/s after varying lengths of time, to a total displacement of 0.2 mm. The strengths of both samples recover nearly identically with time, demonstrating that the recovery depends on time, not displacement. We have previously suggested that this increase in strength mimics the temperature decay, based on a numerical calculation using an infinite half space solution [*Sleep*, 1995]. However, our new finite element calculations (Fig. 10) demonstrate that the temperature decay is much more rapid than indicated by the half space solution, due to the high thermal conductivity components of our sample assembly.

The Nature of the Frictional Weakening Mechanism

Our experiments activate a dramatic frictional weakening mechanism that operates outside the range of displacements available in most rock friction apparatus. Temperature calculations indicate that the observed weakening cannot result from melt lubrication caused by wholesale

melting of the fault surface At higher slip speeds (≥ 75 mm/s) thermal weakening or local melting may occur at the minute contacts between sliding surfaces.

However, the weakening cannot be caused solely by either temperature or large displacement acting alone. Experiments on quartzite at high pressures and temperatures and slow sliding speeds in the triaxial apparatus (to necessarily small displacements) indicate 'normal' values of the friction coefficient of 0.6 or higher [*Stesky*, 1978; *Stesky et al.*, 1974]. These triaxial experiments are conducted at imposed temperatures that span the range of frictionally generated temperatures in our study. The weakening cannot be caused solely by large displacement since experiments to large displacement at low slip speeds (speeds too low to cause significant shear heating) reveal normal friction values (Fig. 1).

We have considered that the weakening may be linked to solid state amorphization, as both quartz and feldspar are susceptible to this effect [*Williams and Jeanloz*, 1988; *Williams and Jeanloz*, 1989]. Transmission electron microscope (TEM) images of friction samples slid at both low [*Yund et al*., 1990] and high speeds [D. Yund, unpublished results] demonstrate that the material is amorphous to electron diffraction. It seems difficult, however, to explain the low strength of the fault material as resulting solely from amorphization; low speed experiments which generate amorphous material [*Yund et al.*, 1990] yield typical values of the friction coefficient. Low speed sliding experiments on silica glass also yield typical friction values [*Weeks et al.*, 1991]. These observations suggest that the strength of the material on the fault is linked to its temperature. Thus, we believe the weakening is caused by profound microstructural changes in the material along the fault that occur with displacement, and shear heating of this highly altered material.

Though we have not yet positively identified this weakening mechanism, we believe it may have important implications for faulting in the earth. Thus, in the Earth, dramatic weakening might occur at conditions much less severe than those required for melting. At higher sliding velocities and normal stresses, we expect a transition to a melt-lubricated regime, which may result in even lower values of the friction coefficient. With our new high-speed sliding capabilities to large displacement at ambient pressure, and our proposed high-speed experiments in our high pressure apparatus, our experimental suite will span the range from quasi-static velocities to truly dynamic slip rates.

Technical advances for attaining high speed at elevated pressure

During the six month no-cost extension on this grant we began the process of designing and purchasing materials to allow future experiments at seismic slip rates and high confining pressure. This is needed in order for us to investigate the process of shear melting. We had previously envisioned attaining these high slip rates of up to 1 m/s by bypassing some of the speed reduction system in our present drive system and replacing it with a sprocket and chain drive system. In this configuration we would still have used our present hydraulic power supply and hydraulic motor that is ultimately powered by a 10 HP electric motor. The problem with this design was that the attainable torque at the required speed was so low that we would have been restricted to relatively low normal stress, and thus the amount of frictional heating would have been substantially lower than is the case for earthquakes. The problem can be seen by noting that the amount of power involved in sliding a sample with our sample dimensions at 1 m/s, a normal stress of 100 MPa, and a coefficient of friction of 0.8 is 79 HP. Clearly our 10 HP motor is inadequate for the task From the scientific perspective, we would like to conduct experiments

with effective normal stress as high as exists at the base of the seismogenic San Andreas fault, ~180 MPa. We would also like to impose a direct step to 1 m/s sliding velocity, since a step to these highest velocities likely occurs at the tip of a propagating earthquake rupture.

We finally decided that the best solution was to purchase a 100 HP motorcycle internal combustion engine and devise a totally new drive system based on it. We were able to obtain at a good price a slightly used 1993 BMW K100RS that had been in an accident that left its mechanical and electrical parts in fine working order, but destroyed enough of the cosmetic parts that it had not been used for several years. It is a 16 valve, four cylinder, water cooled engine that therefore operates smoothly and is suitable for running indoors, as long as the exhaust is vented outdoors. We also purchased most of the other required parts for the drive system, including a high speed right angle gearbox, two pair of "powerchain" sprockets and matching steel-and-fabric belts, and parts for a speed-changer assembly consisting of a brake/clutch assembly and a harmonic drive that allows us to vary the speed over a suitably wide range. When completed, these modifications will allow sliding at slip rates of 10^{-9} to 5×10^{-3} m/s using the existing drive system or slip rates of 10^{-3} to 1 m/s using the new drive system. Alternate drive belts and sprockets will allow even higher speeds. The schematic design of the drive system using these parts has been done, but the detailed design including the drawings to give to our machinist to fabricate the entire assembly will be done in a future year.

Summary

It is apparent from our experiments that substantial reductions in shear stress can occur at slip rates faster than those usually attained in laboratory experiments, even at rates slower than typical of earthquakes and even without frictional melting. The weakening mechanism has not yet been identified. However, our results suggests that dynamic shear stresses could be even lower during faster seismic slip, due whatever process is operative in our experiments. Future studies that involve frictional melting will increase our understanding of another process that should cause dramatic weakening. If large reductions in shear stress are characteristic of earthquakes, it implies that dynamic stress drops may be nearly complete and that accelerations could be quite large unless the initial stress is also small.

FIGURES

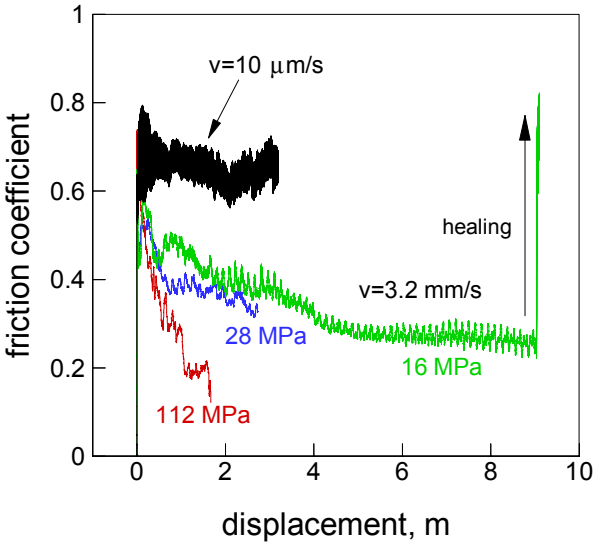

Fig. 1- Plot of friction coefficient vs. displacement for confined samples at normal stresses of 28 and 112 MPa., and effectively unconfined samples at 16 MPa. One sample slid at a normal stress of 28 MPa at 10 µm/s to a displacement of ~3 m did not weaken appreciably. The frictional strength of weakened samples increases to pre-rapid-sliding values with time. All samples were initially slid at 1 µm/s to establish a low-speed baseline for the friction, then at higher speed for the duration of each test.

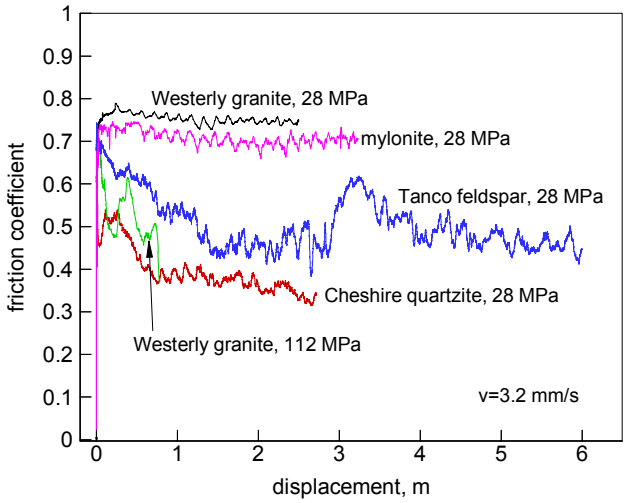

Fig. 2 – Rapid sliding behavior of four different rock types – Westerly granite, quartz mica mylonite, Tanco feldspar, and Cheshire quartzite. Samples were loaded up at a low sliding speed of 1 µm/s, then slid at a velocity of 3.2 mm/s to large displacements. Both granite and mylonite slid at 28 MPa do not weaken with displacement whereas granite slid at 112 MPa weakens similarly to quartzite at 28 MPa.

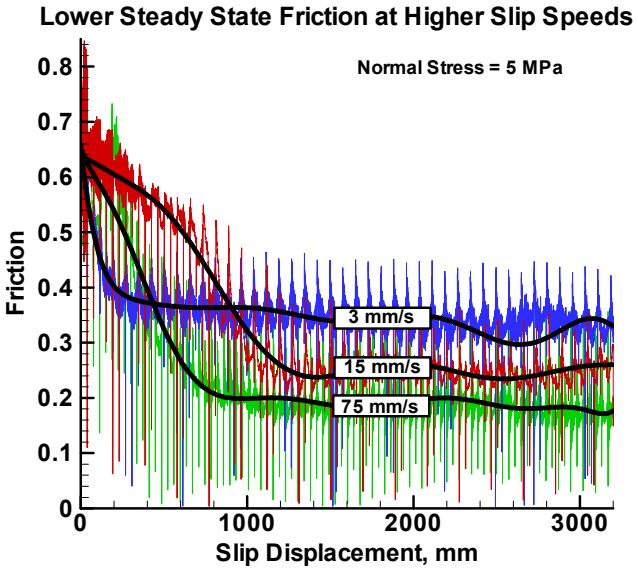

Fig. 3- Large displacements at intermediate slip velocities in unconfined samples. The sliding consisted of many 40 mm increments of rapidly reversed rotation. The sign of the friction has been rectified so it is all plotted as positive. The many vertical spikes occur at the reversals of direction. Tenth order polynomials have been fit to each curve to schematically represent them in Fig 8.

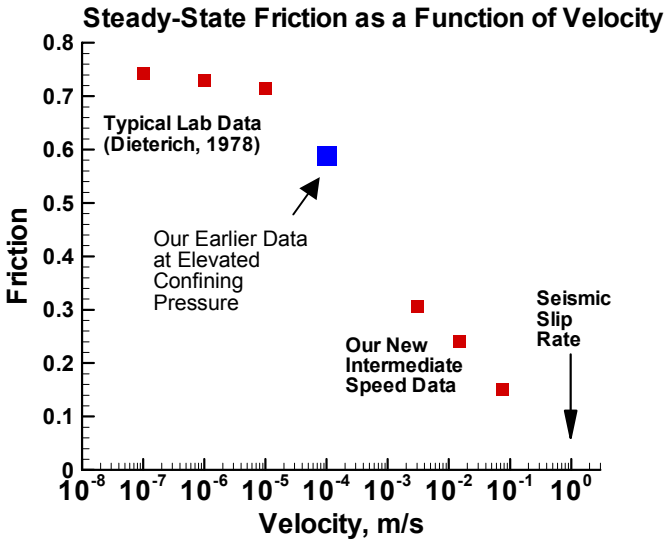

Fig. 4 - Steady-state friction as a function of velocity for our new data compared with typical data for quasi-static experiments. The velocity dependence is much greater at higher velocities. Extrapolating the slope to 1 m/s would give a very low friction, but the slope needs to be better constrained. All the steady-state data we have suggests the same trend.

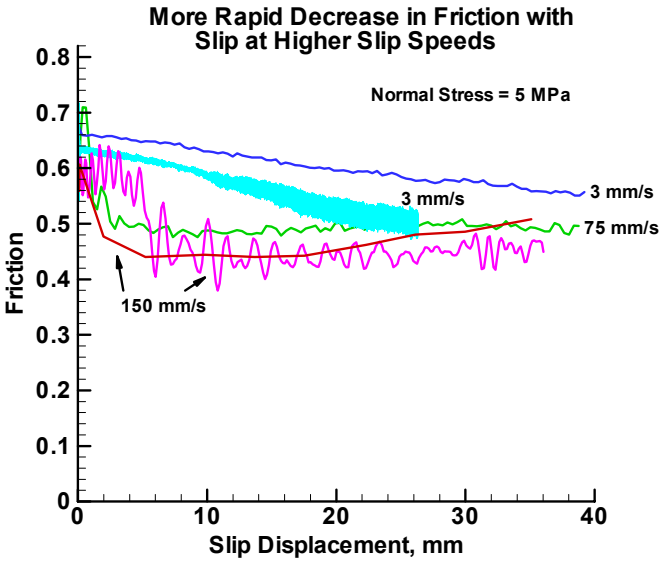

Fig. 5 – Single sliding increments in unconfined samples. The green data at 75 mm/s and the blue data at 3 mm/s are the start of the same colored curves in Fig. 3. The different degrees of detail for the different curves result from widely varying sampling rates, ranging from 40 to 1000 Hz. Given some sample-to-sample variability, the faster sliding rates show systematically more rapid decreases in strength.

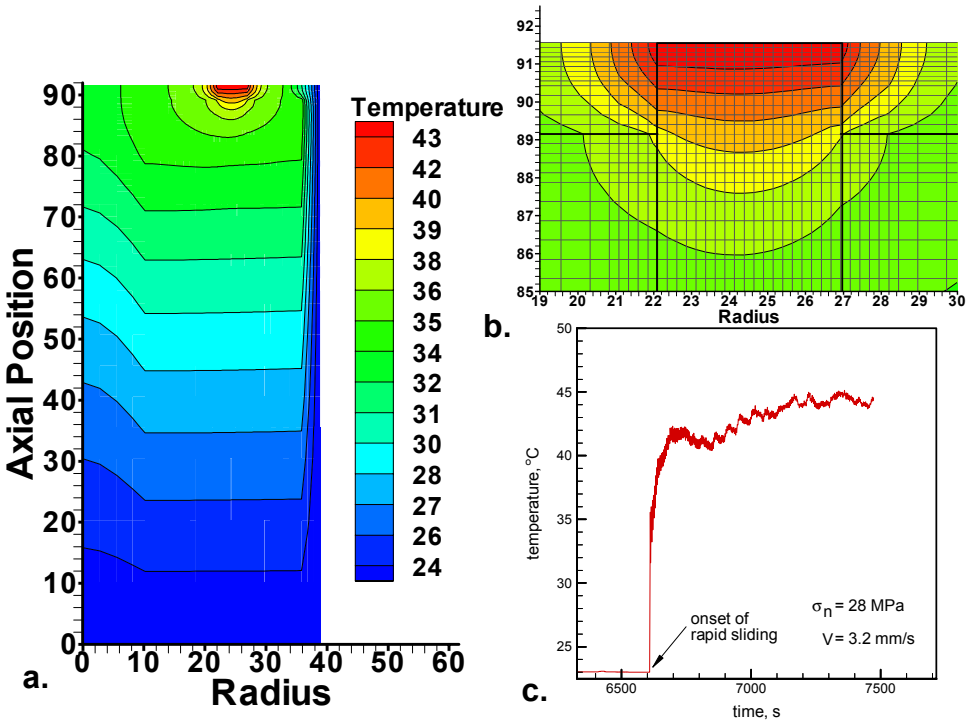

Fig. 6 – a) Plot showing a map of temperatures from our finite element modeling. Shown is a radial longitudinal slice from the axis to the pressure vessel. The area shown in a) is mostly the steel grip and surrounding gas, with sample sliding surface at the top and at a radius of about 25 mm. Representative results for a sliding speed of 3.2 mm/s and a normal stress of 28 MPa are shown.
b) Higher magnification view of the finite element grid near the fault surface. The sample is the central part with radius from 22 to 27 mm. Outside of the sample, the material below the line at 89.2 mm is steel and above the line is Teflon and Viton. c) Plot of temperature vs. time for a node point located at the center of the fault surface.

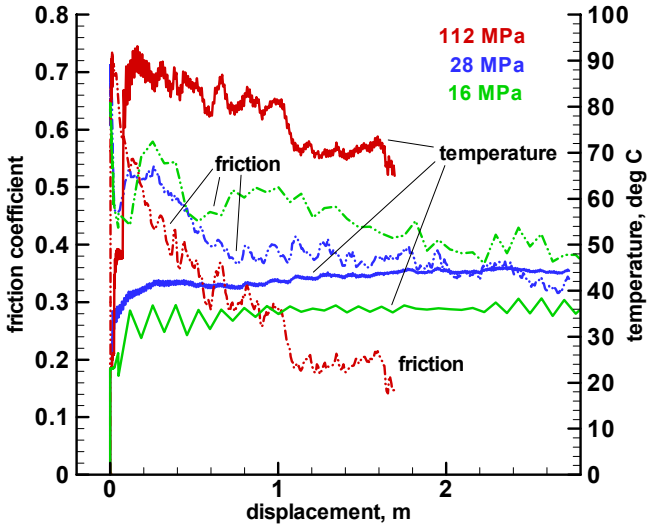

Fig. 7 – Plot of friction coefficient and average surface temperature vs. displacement for rapid sliding at three normal stresses - 16, 28 , and 112 MPa. Temperatures calculated using our finite element model, taking into account time variable friction and sliding velocity.

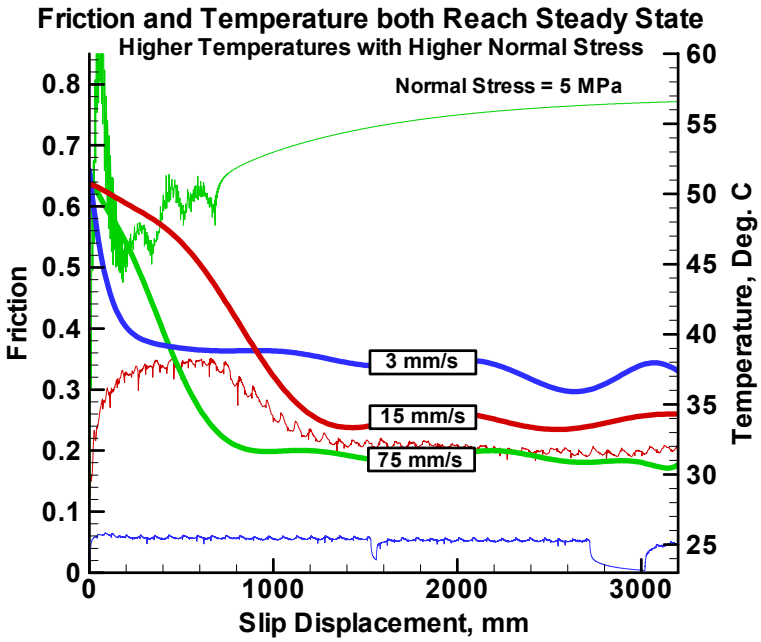

Fig. 8 – Friction coefficient and average surface temperature vs. displacement for rapid sliding at a normal stress of 5 MPa. Temperatures are calculated using our finite element model, taking into account the variations in friction and sliding velocity with time. The labeled smooth curves are the same as the black polynomial fits to the actual friction data of Fig. 3. The color coding is the same in both figures and for both friction and temperature and friction here. The two temperature decays for 3 mm/s occur during periods of no sliding, and the temperature data to their right should be shifted to close these gaps, since no displacement occurs during these times.

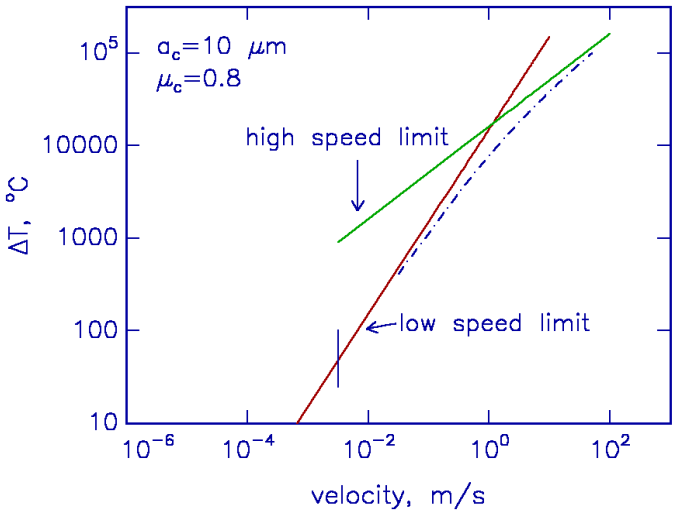

Fig. 9- Calculated "flash" temperatures vs. velocity, after *Archard* (1958). Calculation employs materials parameters for quartz, and assumes a contact size of 10 μm and that the contacts deform plastically, yielding an upper bound for the temperature. Our present maximum slip rate using confining pressure (~3 mm/s) is shown, and is too slow to produce much flash heating.

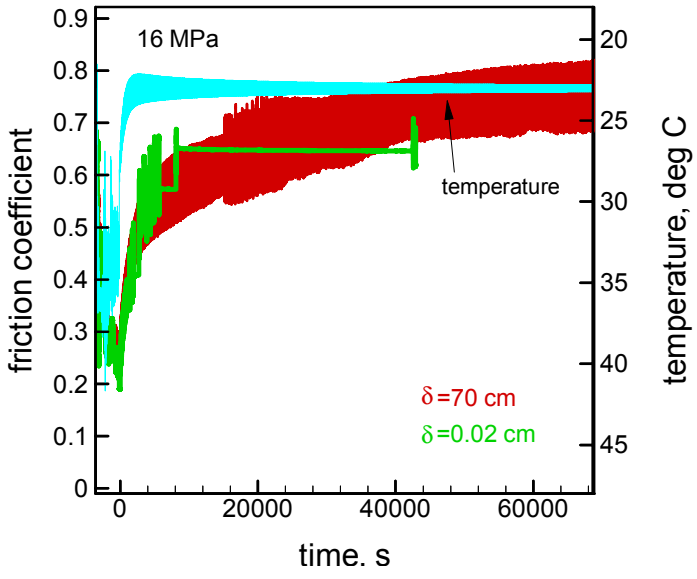

Fig. 10- Strength recovery depends on time, not slip. Plot of friction coefficient and FEM-calculated temperature vs. time for two samples slid at a normal stress of 15.6 MPa. At the cessation of rapid sliding, i.e., at zero time in the figure, one sample was slid continuously at 1 μm/s to a total post-rapid-sliding displacement of 700 mm. The other sample was slid periodically at 1 μm/s after various lengths of time to a total post rapid sliding displacement of 0.2 mm. The similar strengthening with time indicates that healing depends on time, not displacement. Temperature does not seem to explain the slow strength recovery. Strength recovery occurs with a time constant of about 3000 s, much longer than the 400 s time constant of the decrease in temperature, calculated with our finite element model.

REFERENCES CITED

Archard, J.F., The temperature of rubbing surfacess, *Wear*, *2*, 438-455, 1958.

Beeler, N.M., and T.E. Tullis, Self-healing slip pulses in dynamic rupture models due to velocity dependent strength, *Bull. Seis. Soc. Am.*, *86*, 1130-1148, 1996.

Beeler, N.M., T.E. Tullis, M.L. Blanpied, and J.D. Weeks, Frictional behavior of large displacement experimental faults, *Journal of Geophysical Research*, *101*, 8697-8715, 1996.

Ben-Zion, Y., and D.J. Andrews, Properties and implication of dynamic rupture along a material interface, *Bulletin of the Seismological Society of America*, *88*, 1085-1094, 1998.

Beroza, G.C., and P. Spudich, Linearized inversion for fault rupture behavior: application to the 1984 Morgan Hill, California earthquake, *J. Geophys. Res.*, *93*, 6275-6296, 1988.

Bowden, F.P., and D. Tabor, *The Friction and Lubrication of Solids*, 337 pp., Clarendon Press, Oxford, 1964.

Brune, J.N., Tectonic stress and spectra of seismic shear waves from earthquakes, *J. Geophys. Res.*, *75*, 4997-5009, 1970.

Brune, J.N., The physics of earthquake strong motion, in *Seismic Risk and Engineering Decisions*, pp. 141-171, Elsevier, 1976.

Brune, J.N., S. Brown, and P.A. Johnson, Rupture mechanism and interface separation in foam rubber models of earthquakes: a possible solution to the heat flow paradox and the paradox of large overthrusts, *Tectonophysics*, *218*, 59-67, 1993.

Carslaw, H.S., and J.C. Jaeger, *Conduction of Heat in Solids*, 510 pp., Claredon Press, Oxford, 1959.

Cochard, A., and R. Madariaga, Dynamic faulting under rate-dependent friction, *Pure Appl. Geophys*, *142*, 419-445, 1994.

Geller, R.J., D.D. Jackson, Y.Y. Kagan, and F. Mulargia, Earthquakes cannot be predicted, *Science*, *275*, 1616-1617, 1997.

Haskel, N.A., Radiation pattern of surface waves from point sources in a multi-layered medium, *Bulletin of the Seismological Society of America*, *54*, 377-394, 1964a.

Haskel, N.A., Total energy and energy spectral density of elastic wave radiation from propagating faults, *Bulletin of the Seismological Society of America*, *54*, 1811-1841, 1964b.

Haskel, N.A., Total energy and energy spectral density of elastic wave radiation from propagating faults, II, *Bulletin of the Seismological Society of America*, *56*, 125-140, 1966.

Haskel, N.A., Elastic displacements in the near-field of a propagating fault, *Bulletin of the Seismological Society of America*, *59*, 865-908, 1969.

Heaton, T.H., Evidence for and implications of self-healing pulses of slip in earthquake rupture, *Phys. of the Earth and Planetary Interiors*, *64* (1-20), 1990.

Lachenbruch, A.H., Frictional heating, fluid pressure, and the resistance to fault motion, *J. Geophys. Res.*, *85*, 6249-6272, 1980.

Marone, C., and B. Kilgore, Scaling of the critical slip distance for seismic faulting with shear strain in fault zones, *Nature*, *362*, 618-621, 1993.

Mase, C.W., and L. Smith, Pore-fluid pressures and frictional heating on a fault surface, *J. Geophys. Res.*, *92* (B7), 583-607, 1984.

Mase, C.W., and L. Smith, Effects of frictional heating on the thermal hydrologic and mechanical response of a fault, *Journal of Geophysical Research*, *92*, 6097-6112, 1987.

Melosh, H.J., Acoustic fluidization: A new geologic process?, *J. Geophys. Res.*, *84*, 7513-7520, 1979.

Melosh, J., Dynamic weakening of faults by acoustic fluidization, *Nature*, *397*, 601-606, 1996.

Perrin, G.O., J.R. Rice, and G. Zheng, Self-healing slip pulse on a frictional surface, *Joural of Mechanics and Physics of Solids*, *43* (9), 1461-1495, 1994.

Rice, J.R., Flash heating at asperity contacts and rate-dependent friction, *Eos Transactions of the American Geophysical Union*, *80*, F681, 1999.

Segall, P., and J.R. Rice, Dilatancy, compaction, and slip instability of a fluid infiltrated fault, *Journal of Geophysical Research*, *100*, 22155-22173, 1995.
Sleep, N.H., Frictional heating and the stability of rate and state dependent frictional sliding, *Geophysical Research Letters*, *22*, 2785-2788, 1995.
Spray, J.G., Artificial generation of pseudotachylite using friction welding apparatus: simulation of melting on a fault plane, *J. Struct. Geol.*, *9*, 49-60, 1987.
Stesky, R.M., Mechanisms of high temperature frictional sliding in Westerly granite, *Can. J. Earth Sciences*, *15*, 361-375, 1978.
Stesky, R.M., W.F. Brace, D.K. Riley, and P.-Y.F. Robin, Frictionm in faulted rock at high temperature and pressure, *Tectonphysics*, *23*, 177-203, 1974.
Tsutsumi, A., and T. Shimamoto, High-velocity frictional properties of gabbro, *Geophysical Research Letters*, *24*, 699-702, 1997.
Weeks, J.D., N.M. Beeler, and T.E. Tullis, Frictional behavior: glass is like a rock, *Journal of Geophysical Research*, *72*, 357-458, 1991.
Williams, Q., and R. Jeanloz, Coordination changes in glasses and static amorphization of crystalline silicates at high-pressure, *Chemical Geology*, *70*, 91, 1988.
Williams, Q., and R. Jeanloz, Static amorphization of anorthite at 300-K and comparison with diaplectic glass, *Nature*, *338*, 413-415, 1989.
Yund, R.A., M.L. Blanpied, T.E. Tullis, and J.D. Weeks, Amorphous material in high strain experimental fault gouges, *J. Geophys. Res.*, *95*, 15589-15602, 1990.

GRANT NUMBER: 00-HQGR0050

LABORATORY EXPERIMENTS ON ROCK FRICTION FOCUSED ON UNDERSTANDING EARTHQUAKE MECHANICS

Terry E. Tullis and David L. Goldsby

Brown University, Department of Geological Sciences, Providence RI 02912-1846

Tele: (401) 863-3829, FAX: (401) 863-2058, Email: Terry_Tullis@brown.edu
Web Site. http://www.geo.brown.edu/faculty/ttullis/index.html

NEHRP Element III - Understanding Earthquake Processes

Key Words: Laboratory studies, Source characteristics, Fault dynamics, Strong ground motion

NON-TECHNICAL ABSTRACT

We have measured the frictional resistance of rock and find that if slip is fast enough, the fault can weaken much more dramatically than extrapolation of lower velocity results would have implied. The strength extrapolates to nearly zero at earthquake slip rates. The reason for this is not clear, but the temperatures resulting from the frictional heating are too low to have produced melting. This low resistance could cause unexpectedly strong shaking of the ground and potentially more severe damage than currently expected.